



Demagnetization of Ordinary Chondrites under Hydrostatic Pressure up to 1.8 GPa

N. Bezaeva, J. Gattacceca, Pierre Rochette, R. Sadykov

► To cite this version:

N. Bezaeva, J. Gattacceca, Pierre Rochette, R. Sadykov. Demagnetization of Ordinary Chondrites under Hydrostatic Pressure up to 1.8 GPa. *Geochemistry International / Geokhimiya*, 2022, 60 (5), pp.421-429. 10.1134/S0016702922050032 . hal-03565123

HAL Id: hal-03565123

<https://hal.science/hal-03565123>

Submitted on 10 Feb 2022

HAL is a multi-disciplinary open access archive for the deposit and dissemination of scientific research documents, whether they are published or not. The documents may come from teaching and research institutions in France or abroad, or from public or private research centers.

L'archive ouverte pluridisciplinaire **HAL**, est destinée au dépôt et à la diffusion de documents scientifiques de niveau recherche, publiés ou non, émanant des établissements d'enseignement et de recherche français ou étrangers, des laboratoires publics ou privés.

Demagnetization of Ordinary Chondrites under Hydrostatic Pressure up to 1.8 GPa

© 2021 N. S. Bezaeva^{a*}, J. Gattacceca^{b**}, P. Rochette^{b***}, R. A. Sadykov^{c****}

^a*Vernadsky Institute of Geochemistry and Analytical Chemistry,
Russian Academy of Sciences, 19 Kosygin Str., Moscow, 119991 Russia*

*email: bezaeva@geokhi.ru

^b*CNRS, Aix Marseille Univ, IRD, INRAE, BP80, 13545, Aix-en-Provence, France*

email: gattacceca@cerege.fr; *email: rochette@cerege.fr

^c*Institute for Nuclear Research, Russian Academy of Sciences,
Prospekt 60-letiya Oktiabria 7a, 117312, Moscow, Russia*

****email: rsadykov@inr.ru

Abstract—We present here the results of hydrostatic pressure demagnetization experiments up to 1.8 GPa on LL, L and H ordinary chondrites - the most common type of meteorites with Fe-Ni alloys being the main magnetic carrier. We used a non-magnetic high-pressure cell of piston-cylinder type made of "Russian" alloy (NiCrAl) together with a liquid pressure transmitting medium PES-1 (polyethylsiloxane) to ensure purely hydrostatic pressure. This technique allowed measuring magnetic remanence of investigated samples directly under pressure as well as upon decompression. Pressure was always applied in near-zero magnetic field ($< 5 \mu\text{T}$). The experiments revealed that under hydrostatic pressure up to 1.8 GPa, ordinary chondrites lose up to 51% of their initial saturation isothermal remanent magnetization. Pressure demagnetization degree is directly proportional to the coercivity of remanence (B_{cr}), which reflects the magnetic hardness of the samples. This is similar to what was observed for ferrimagnetic minerals others than Fe-Ni alloys. In addition, pressure of 1.8 GPa does not demagnetize samples with $B_{\text{cr}} > 80$ mT, i.e. whose main metal phase is tetrataenite ($\text{Fe}_{0.5}\text{Ni}_{0.5}$). This study gives an overview of pressure sensitivity of ordinary chondrites up to 1.8 GPa and has implications for extraterrestrial paleomagnetism as it can help to interpret remanent magnetization of ordinary chondrites that suffered shock metamorphism processes.

Keywords: ordinary chondrites, pressure demagnetization, magnetic properties, hydrostatic pressure

INTRODUCTION

Hypervelocity impacts represent a fundamental process in the evolution of the solid matter in the Solar System. Shock waves generated during impacts modify the target rocks and minerals in a unique way and can also erase or overprint the magnetic record of the Solar System solid bodies (Mars, Moon, asteroids...), a record that can be studied in meteorites (Weiss et al., 2010). Fe-Ni is known to be the main magnetic carrier in most groups of meteorites (Lauretta and McSween, 2006). Interpretation of paleomagnetic data of extraterrestrial materials and, in particular, the search of primary magnetizations, acquired in the early Solar System, require the knowledge of the shock effects on remanent magnetism of Fe-Ni-bearing meteorites. Laboratory shock experiments are characterized by the difficulty in calibrating shock pressure, and possible mechanical damages of investigated samples (e.g. Fuller et al., 1974; Bezaeva et al., 2016a; Badyukov et al., 2018). Static pressure experiments allow better pressure calibration and are essentially non-destructive for samples. Until recently, such experiments were characterized by a limited pressure range, non-hydrostatic load and limited sample volume, which allowed working only on individual magnetic grains rather than bulk rocks (e.g. Gilder and LeGoff, 2008). However, it is important to study bulk samples representative of natural processes. This requires relatively large sample volumes to be allowed in the pressure chamber. Bezaeva et al. (2010) used bulk samples to investigate hydrostatic pressure demagnetization effect up to 1.2 GPa in a wide range of rocks and magnetic minerals, including Fe-Ni alloys. However, the set of Fe-Ni-bearing samples in (Bezaeva et al., 2010) was restricted to only three ordinary chondrites (OC) with a variable but limited range of magnetic hardness values, expressed by the coercivity of remanence B_{cr} . This manuscript is a follow up study on hydrostatic pressure demagnetization of a larger set of ordinary chondrites and over a more extended pressure range.

The main objective of this study is to quantify experimentally the magnetic remanence sensitivity of a more representative set of OCs with B_{cr} spanning three orders of magnitude (5 to 400 mT) to hydrostatic load up to 1.8 GPa.

MATERIALS AND METHODS

Sample description

For this study, we preselected nine pristine samples of OC from the LL, L and H groups (Abreu, 2018), with a particularly wide range of remanent coercivity values B_{cr} from 5 to 404 mT (Table 1).

Table 1. Bulk magnetic properties of ordinary chondrite samples used in this study

meteorite	Sample #	Type	m	M_{rs}	M_s	M_{rs}/M_s	B_{cr}	B_c	B_{cr}/B_c
Lançon	1108	H6	84.6	243	41570	0.006	5.4	0.7	8.2
Agen	139	H5	121.0	49	8470	0.006	10.8	1.3	8.4
Pultusk	2713	H5	61.9	303	42680	0.007	26.8	1.0	25.9
Savtschenskoe	2476	LL4	25.5	53	5410	0.010	45.5	2.6	17.4
Ochansk	2675	H4	61.5	392	42950	0.009	46.0	1.3	34.7
Jelica	2597	LL6	90.4	84	970	0.087	78.0	32.6	2.4
Adzi-Bogdo	3174	LL3-6	85.5	180	2640	0.068	91.6	22.1	4.1
L'Aigle	9	L6	145.7	353	13650	0.026	225.2	6.6	33.9
Guider	2261	LL5	47.4	452	1298	0.349	403.5	151.8	2.7

Note: m is mass (in mg); M_{rs} is saturation remanent magnetization (in mAm^2/kg); M_s is saturation magnetization in mAm^2/kg ; B_c is coercivity and B_{cr} is remanent coercivity (in mT).

The OC samples were all falls (W0, i.e. pristine without traces of terrestrial weathering) and included Lançon (H6), Agen (H5), Pultusk (H5), Savtschenskoe (LL4), Ochansk (H4), Jelica (LL6), Adzi-Bogdo (LL3-6), L'Aigle (L6), Guider (LL5). The samples for this study were provided by the French Muséum National d'Histoire Naturelle (Paris, France). As mentioned above, typical magnetic remanence carriers in OCs are metallic Fe-Ni alloys with different nickel content: taenite (Ni ~ 30-50 wt.%, face-centered cubic structure, fcc), tetrataenite (Ni ~ 50 wt.%, tetragonal structure) and kamacite (Ni ≤ 7 wt.%, body-centered cubic structure, bcc) (Sugiura and Strangway, 1988; Gattacceca et al., 2014).

Experimental equipment and protocols

All magnetic measurements were carried out at CEREGE (Aix-en-Provence, France). We used Princeton Micromag Vibrating Sample Magnetometer (VSM) with maximum applicable magnetic field of 1 T and a moment sensitivity of $\sim 10^{-8} \text{ Am}^2$ for measurements of hysteresis loops and backfield remanence demagnetization curves at room temperature. Coercivity B_c , remanent coercivity B_{cr} , saturation remanent magnetization M_{rs} , saturation magnetization M_s are presented in Table 1.

Pressure demagnetization experiments were carried out using a nonmagnetic high-pressure cell of piston-cylinder type (Sadykov et al., 2009) allowing direct measurements in a 2G Enterprises SQUID (Superconducting Quantum Interference Device) magnetometer (model

755R). Magnetic moments up to 10^{-4} Am^2 can be measured with a practical background noise level of 10^{-11} Am^2 . The pressure cell has several modifications with regard to the cell described by Sadykov et al. (2008): it is entirely made of “Russian alloy” ($\text{Ni}_{57}\text{Cr}_{40}\text{Al}_3$), its inner diameter is 8 mm and the maximum applicable calibrated pressure is 1.8 GPa. Moreover, the teflon plug, described in Sadykov et al. (2008), was replaced by a special inner piston-plug made of “Russian alloy” with a CuBe antiextrusion gasket. The reported (actual) pressure values are 10% less with regard to the external load (for details see Sadykov et al., 2008, 2009; Bezaeva et al., 2010, 2016b). The pressure cell was intercalibrated with the previous one used by Bezaeva et al. (2010) (see figure caption for Fig. 1).

We used the following protocol for all pressure demagnetization experiments. After acquisition of saturation isothermal remanent magnetization (SIRM) in a 3 T magnetic field using pulse magnetizer MPM9 from Magnetic Measurements Ltd., the sample was placed into a teflon capsule, filled with inert polyethylsiloxane (PES-1) liquid and locked with a special piston-plug. PES-1 allows converting the uniaxial pressure on the pistons into a pure hydrostatic pressure on the sample (Kirichenko et al., 2005). After loading of the cell with a press Graseby Specac 15011, pressure inside the cell was locked by clamping. In order to isolate pressure demagnetization effect on remanent magnetization and exclude the creation of piezoremanent magnetization (PRM) after pressure application (studied in many previous works e.g. Nagata and Kinoshita, 1965; Nagata, 1966; Kinoshita, 1968; Nagata et al., 1982), in this work pressure was always applied in ambient magnetic field that was low enough ($<5 \mu\text{T}$) to be considered negligible in view of the starting remanence acquired in a strong field (3 T). For this, the press with the cell inside was placed at the center of three pairs of perpendicular Helmholtz coils connected to stabilized DC supplies. Due to the presence of mobile metallic parts in the press, it was not possible to obtain a stable lower ambient field. The magnetic field in the area of the investigated sample was monitored using a 3 axis flux-gate magnetometer and was always $<5 \mu\text{T}$. Thus, in these experiments, any possible PRM acquisition was negligible compared to the pressure demagnetization. We used 11-step pressure demagnetization protocol, which is specified in Table 2.

The magnetic moment of the sample under pressure and upon decompression was measured at each pressure step up to 1.8 GPa using the above-described SQUID magnetometer. The remanence of the empty pressure cell at ambient pressure and room temperature is $\sim 3 \times 10^{-8} \text{ Am}^2$; at each subsequent pressure step up to 1.8 GPa it was always at least two orders of magnitude lower than the remanence of the investigated sample (with the exception of

Savtschenskoe, for which at final pressure steps the sample remanence was only ~30 times higher than the cell remanence). Thus, there was no need for correction of the magnetic remanence of the sample by the magnetic remanence of the cell.

After decompression, the sample was extracted from the cell and demagnetized by alternating field (AF), then resaturated in a 3 T magnetic field and demagnetized by AF again. In this study, median destructive field (MDF_i) is defined as the alternating magnetic field needed to reduce SIRM by half.

RESULTS AND DISCUSSION

Pressure demagnetization experiments up to 1.8 GPa were reproducible, mechanically non-destructive (with an exception of Guidder, for which a small piece of ~25% of the initial mass split off after pressure demagnetization experiment), and did not change the bulk magnetic properties of investigated samples (e.g., M_{rs} etc., see Table 1). The latter is in agreement with the fact that there is no magnetic phase transitions in Fe-Ni-bearing ferrimagnetic minerals in the given pressure range (Wei and Gilder, 2013; Wei et al., 2017).

Figure 1 displays normalized isothermal remanent magnetization (IRM) versus hydrostatic pressure (p) from $p = 0$ ($IRM_{p=0} = SIRM$) up to 1.8 GPa for all investigated ordinary chondrite samples. Related experimental data are presented in Table 2. As seen from Fig. 1, pressure application up to 1.8 GPa resulted in demagnetization of samples, i.e. a decrease of their IRM. This decrease is irreversible, i.e. IRM does not recover upon decompression. Pressure demagnetization degree Δ is defined as follows:

$$\Delta = (1 - IRM_{pmax}/SIRM) \times 100\% \quad (1),$$

where IRM_{pmax} is defined as IRM under 1.8 GPa. Δ is expressed in %. $\Delta=0\%$ for no pressure demagnetization at all, and $\Delta=100\%$ for total pressure demagnetization.

Δ under maximum pressure varies from 1 to 51%. Values of Δ under maximum pressure and its variations upon decompression (δ , defined as changes in IRM upon decompression in % from SIRM) are presented in Table 3. The maximum pressure demagnetization degree (~50%) is observed for the samples of Lançon and Agen with the lowest values of remanent coercivity B_{cr} . This is in agreement with the previously published statement that within the same class of magnetic minerals (Fe-Ni in this paper) pressure demagnetization degree is mainly controlled by the magnetic hardness of the samples (Bezaeva et al., 2010).

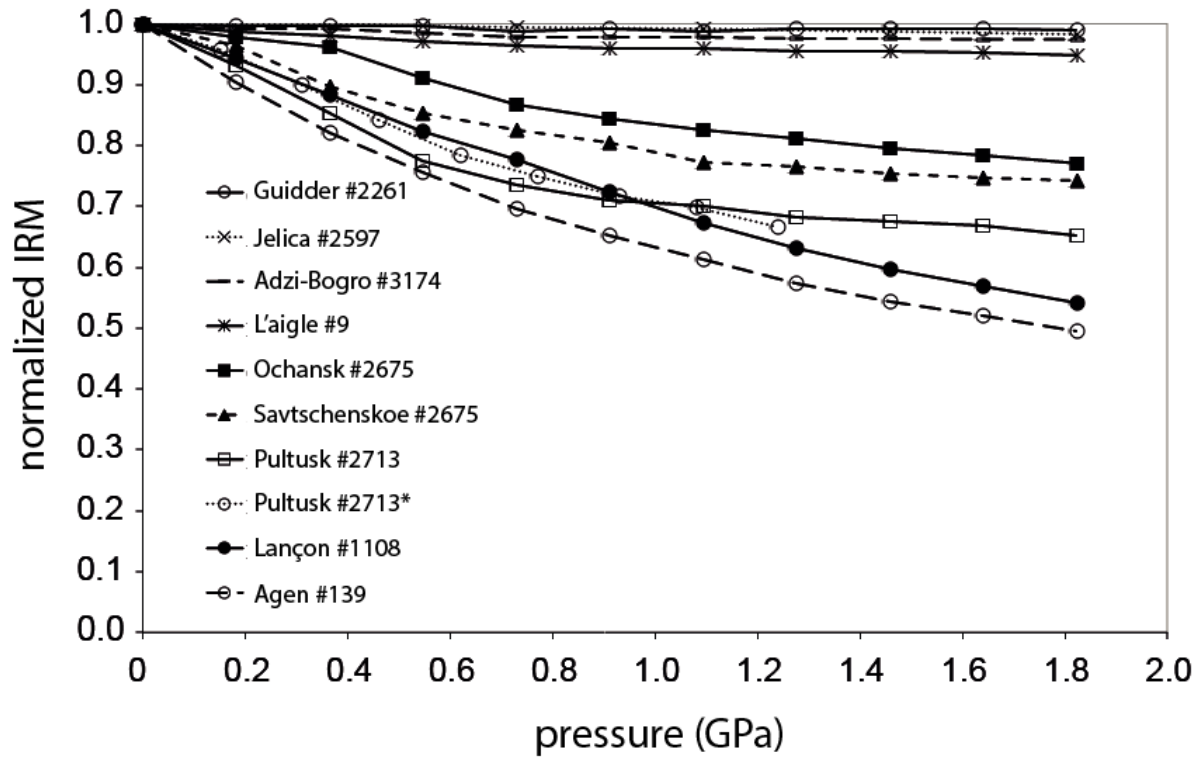


Figure 1. Isothermal remanent magnetization IRM, normalized to SIRM versus hydrostatic pressure up to 1.8 GPa for ordinary chondrite samples. Pultusk #2713* corresponds to pressure demagnetization curve up to 1.24 GPa for the same Pultusk sample, previously published in (Bezaeva et al., 2010) and presented here for comparison.

Table 2. Experimental data from pressure demagnetization experiments (Figure 1).

Meteorite	Lançon	Agen	Pultusk	Savtsch.	Ochansk	Jelica	Adzi-B.	L'Aigle	Guidder
#	p	IRM _p *	IRM _p *	IRM _p *	IRM _p *	IRM _p *	IRM _p *	IRM _p *	IRM _p *
1	0.00	1.00	1.00	1.00	1.00	1.00	1.00	1.00	1.00
2	0.18	0.94	0.90	0.93	0.96	0.98	1.00	0.99	1.00
3	0.36	0.88	0.82	0.85	0.90	0.96	1.00	0.99	1.00
4	0.55	0.82	0.76	0.78	0.85	0.91	1.00	0.99	1.00
5	0.73	0.78	0.70	0.74	0.82	0.87	0.99	0.98	0.99
6	0.91	0.72	0.65	0.71	0.80	0.84	-	0.98	0.99
7	1.09	0.67	0.61	0.70	0.77	0.83	0.99	0.98	0.99
8	1.28	0.63	0.57	0.68	0.76	0.81	-	0.98	0.99
9	1.46	0.60	0.54	0.68	0.75	0.80	0.99	0.98	0.99
10	1.64	0.57	0.52	0.67	0.75	0.78	-	0.97	0.99
11	1.82	0.54	0.49	0.65	0.74	0.77	0.98	0.97	0.99

12	0.00	0.57	0.43	0.66	0.69	0.73	0.99	0.97	0.96	0.99
----	------	------	------	------	------	------	------	------	------	------

Note: all pressure steps in 12-step experimental protocol are numbered consecutively in the left column, see Materials and Methods; p is calibrated pressure in GPa; *Savtsch.* is Savtschenskoe. *Adzi-B.* is Adzi-Bogdo; $IRM_p^* = IRM_p / SIRM$, IRM_p is isothermal remanent magnetization under pressure, $SIRM$ is saturation isothermal remanent magnetization.

As seen from Fig. 1, pressure demagnetization curves have slightly different shapes. Following Bezaeva et al. (2010), we calculated α parameter for all our samples (see Table 3). This parameter, describing the shape of the pressure demagnetization curve, is defined as follows:

$$\alpha = [(SIRM - IRM_{p_l}) / (SIRM - IRM_{p_{max}})] / [p_l / p_{max}] \quad (2),$$

where IRM_{p_l} is IRM under $p_l = 0.73$ GPa and $IRM_{p_{max}}$ is IRM under $p_{max} = 1.82$ GPa.

If we exclude three samples with $\Delta < 5\%$ (Table 3), α values vary from 1.2 to 1.9 with a mean value of 1.6 ± 0.2 indicating concave shape of pressure demagnetization curves, in accordance with previous findings (Bezaeva et al., 2010).

Table 3. Results of pressure demagnetization experiments

meteorite	MDF _i	Δ	δ	α	ε_1	ε_0
Lançon	2	46	3	1.2	-	-
Agen	6	51	-7	1.5	65	55
Pultusk	17	35	1	1.9	87	31
Savtschenskoe	18	26	-5	1.7	94	26
Ochansk	19	23	-4	1.5	91	20
Jelica	24	2	1	0.8	69	3
Adzi-Bogdo	35	3	0	2.1	53	11
L'Aigle	107	5	1	1.7	55	12
Guider	233	1	-1	3.4	-	-

Note: $p_l = 0.73$ GPa; $p_{max} = 1.82$ GPa; MDF_i is median destructive field of saturation isothermal remanent magnetization (in mT); extrapolated values of MDF_i (not reached experimentally) are italicized; Δ (in %) is pressure demagnetization degree under maximum pressure (1.82 GPa); δ (in %) corresponds to changes in isothermal remanent magnetization (IRM) upon decompression from 1.82 GPa (IRM decreases when δ is negative and increases when δ is positive); $\alpha = [(SIRM - IRM_{p_l}) / (SIRM - IRM_{p_{max}})] / [p_l / p_{max}]$, where $SIRM$ is saturation IRM before compression in the pression cell, IRM_{p_l} is IRM under p_l and $IRM_{p_{max}}$ is IRM under p_{max} ;

$\varepsilon_1 = 1 - \varepsilon(30\text{mT})/\varepsilon_0$, where $\varepsilon(\text{AF}) = [\text{SIRM}_{\text{AF}}(\text{AF}) - \text{IRM}_{\text{AFp}}(\text{AF})]/\text{SIRM}_{\text{AF}}(\text{AF}) \times 100\%$, $\varepsilon_0 = \varepsilon(0\text{mT})$; AF is alternating magnetic field (see text); SIRM_{AF} and IRM_{AFp} correspond to IRM values before and after pressure application, respectively, so that $\text{SIRM}_{\text{AF}}(\text{AF})$ curve is a curve of AF demagnetization of SIRM and $\text{IRM}_{\text{AFp}}(\text{AF})$ is a curve of AF demagnetization of residual IRM after decompression from 1.82 GPa and extraction of the sample from the cell.

Figure 2 displays normalized IRM versus B_{cr} for three different pressure values ($p_1=0.18$ GPa; $p_4=1.28$ GPa; $p_{\text{max}}=1.82$ GPa): actual data (Figs 2a-c) and linear fits (Figs 2d-f) for data points prior to 'plateau' effect (see below). Figure 3 displays five linear fits, the corresponding parameters being given in Table 4. These linear fits are characterized by coefficient of determination R^2 values ranging from 0.78 to 0.97. Bezaeva et al. (2010) showed that within the same family of magnetic minerals there exists a correlation between Δ and the magnetic hardness of the sample (B_{cr}). As seen from Figure 3 such correlation holds but is better described by a different type of equation.

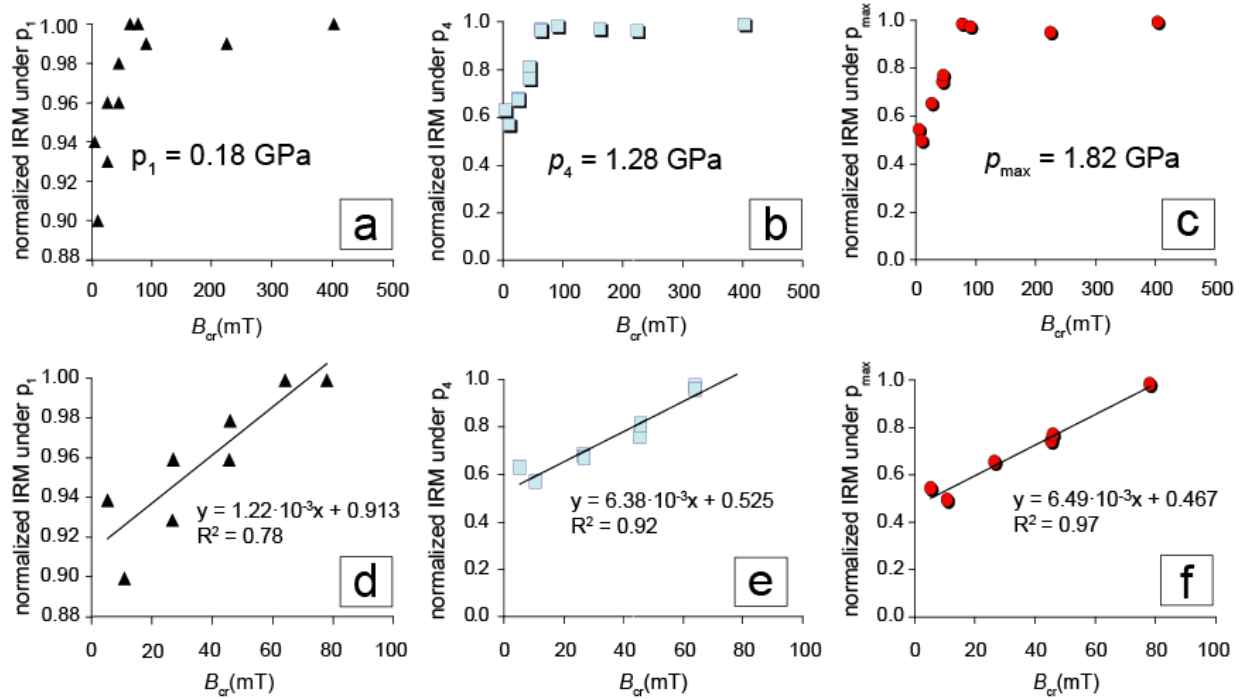


Figure 2. Empirical dependency of isothermal remanent magnetization under hydrostatic pressure p versus remanent coercivity B_{cr} for ordinary chondrites. Figs 2a-c display all available data for $p_1=0.18$ GPa, $p_4=1.28$ GPa and $p_{\text{max}}=1.82$ GPa, respectively. Figs 2a-b also include pressure demagnetization data from Bezaeva et al. (2010) acquired on Pultusk, Bensour and Saratov ordinary chondrites. For $B_{\text{cr}} > 80$ mT there is a “plateau” effect and pressure demagnetization no longer occurs in the given pressure range. And

prior to ‘plateau’ there is a linear dependence between normalized IRM under pressure and B_{cr} , which is well expressed in Figs 2d, 2e and 2f.

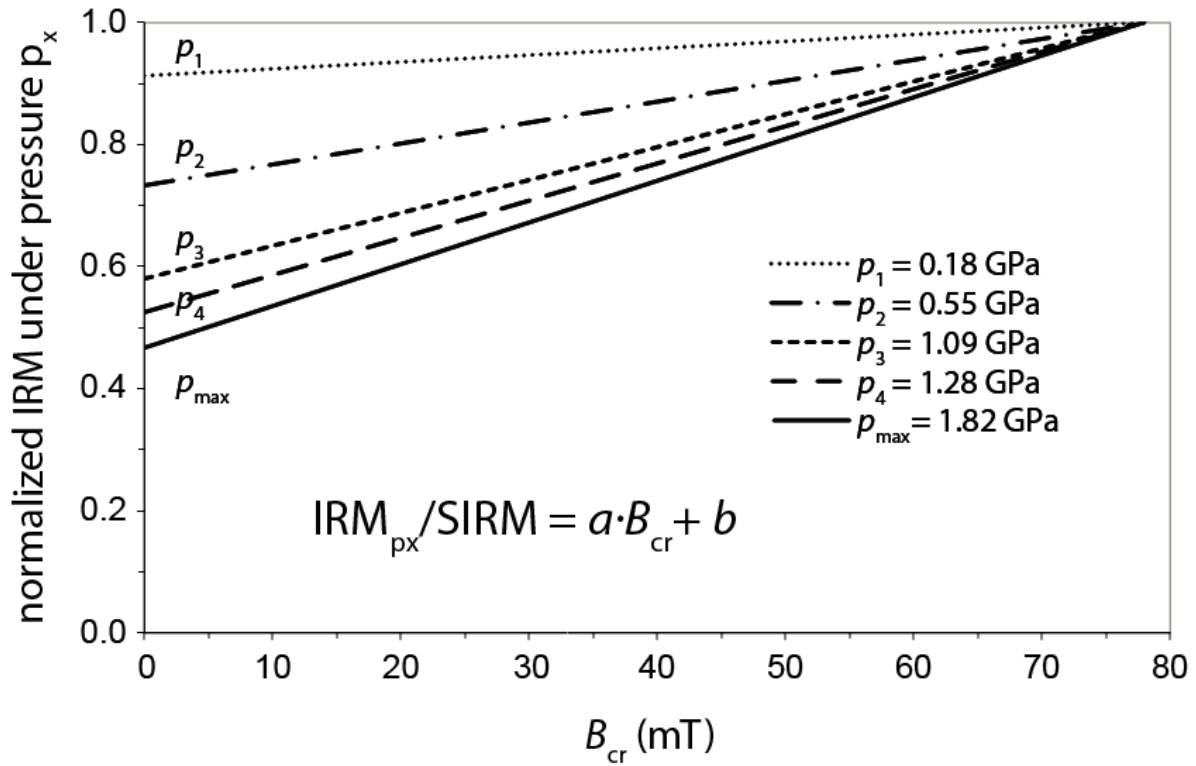


Figure 3. Empirical dependency of normalized isothermal remanent magnetization ($IRM_{px}/SIRM$) under hydrostatic pressure p_x ($x=1,2,3\dots$) versus remanent coercivity B_{cr} for Fe-Ni-bearing ordinary chondrites. This graph gives a predictive model, which can be used to determine the degree of pressure demagnetization of Fe-Ni-bearing samples for given pressure and B_{cr} values with 5% accuracy.

Table 4. Fitting parameters for Figures 2-3.

#	p	a	b	R^2
p_1	0.18	1.22×10^{-3}	0.913	0.78
p_2	0.55	3.34×10^{-3}	0.733	0.81
p_3	1.09	5.20×10^{-3}	0.580	0.93
p_4	1.28	6.38×10^{-3}	0.525	0.92
p_{max}	1.82	6.49×10^{-3}	0.467	0.97

Note: p is pressure in GPa; a (in mT^{-1}) and b (dimensionless) are linear fit coefficients; R^2 is determination coefficient reflecting the confidence of chosen approximation.

Indeed, our new experimental data on a larger dataset allow a better description of the relationship between pressure demagnetization and coercivity of remanence:

$$\text{IRM}_{\text{px}}/\text{SIRM} = aB_{\text{cr}} + b \quad (3),$$

where B_{cr} is remanent coercivity in mT; a (in mT^{-1}) and b (dimensionless) are fitting parameters (see Fig. 2 and Table 4); $[\text{IRM}_{\text{pmax}}/\text{SIRM}] \times 100\% = 100 - \Delta$.

As seen from Figures 1 and 3, Δ , calculated for different pressure values using equation (1), increases with increasing pressure. Figure 3 can be considered as a predictive empirical model for five given pressure values, and can be used to determine the degree of pressure demagnetization of Fe-Ni-bearing samples for given p and B_{cr} values ($p \leq 1.8$ GPa) with 5% accuracy. Similar dependencies can be plotted for any other hydrostatic pressure values from 0 to 1.8 GPa range. This predictive model can be applied to ordinary chondrite samples as well as any other Fe-Ni-bearing samples (e.g. iron meteorites).

We also determined a threshold B_{cr} value (further referred to as $B_{\text{cr-th1}}$), above which there is a ‘plateau’ effect and no further pressure demagnetization occurs in the given pressure range. For Fe-Ni magnetic mineralogy and $p = 1.8$ GPa, $B_{\text{cr-th1}} = 80$ mT (Fig. 2). This is in agreement with previous findings (Bezaeva et al., 2010). Indeed, Bezaeva et al. (2010) investigated a group of Fe-Ni-bearing samples (also OC) and found that for $p = 1.24$ GPa threshold value $B_{\text{cr-th2}} \approx 70$ mT. The slight difference between $B_{\text{cr-th1}}$ and $B_{\text{cr-th2}}$ values is likely due to higher number of samples and/or higher-pressure range used in this study. Taking into account the degree of pressure demagnetization Δ of Fe-Ni-bearing OC samples (Bensour, Pultusk, Saratov) under 1.24 GPa, reported in (Bezaeva et al., 2010), Δ values under $p_4=1.28$ GPa for OC samples in this study (Table 1) and a linear character of Δ versus B_{cr} dependence, we could refine the $B_{\text{cr-th}}$ value under 1.2 GPa to $B_{\text{cr-th2}}=74$ mT. This latter value comes from a larger dataset and thus is likely to be more accurate.

It is worth pointing out to the behavior of remanence after decompression. Indeed, Bezaeva et al. (2010) showed that upon decompression residual remanent magnetization of different magnetic minerals can exhibit no further changes or change both towards a further decrease as well as a recovery with regard to Δ under pressure (see δ values in Table 3). Moreover, remanence behavior pattern upon decompression depends on the specific magnetic mineral: application of pressure up to 1.24 GPa to Fe-Ni bearing samples (OC) resulted in the variation of δ within $[-4; 2]\%$ range with regard to initial pre-compression SIRM value ($\delta = -6\%$ for a sample of powdered iron Fe^0 dispersed in epoxy, see Bezaeva et al., 2010). This study confirms such trend however reveals slightly larger amplitude of δ variations: from -6% to $+3\%$.

Thus, the typical behavior of remanence for Fe-Ni-bearing samples upon decompression are slight variations towards further decrease or recovery of remanence, whose absolute value does not exceed 6% from initial value of pre-compressed SIRM of the sample (Table 3).

Figure 4 displays AF demagnetization curves of SIRM for all nine samples.

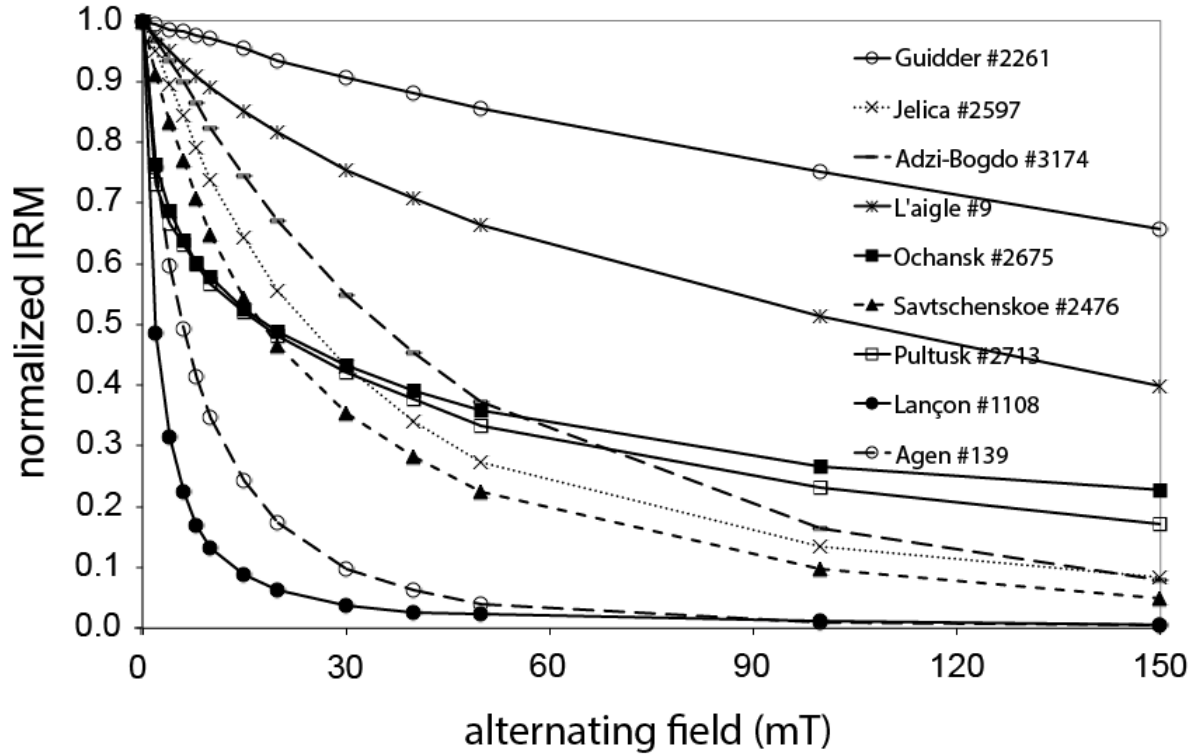


Figure 4. Alternating field demagnetization of saturation isothermal remanent magnetization (normalized to its initial value).

As follows from Fig.4, samples with similar AF demagnetization pattern (e.g., Ochansk and Pultusk) may have very different pressure demagnetization patterns: $\Delta = 23\%$ for Ochansk and $\Delta = 35\%$ for Pultusk (Fig. 1). Conversely, samples with very different AF demagnetization pattern (e.g. Adzi-Bogdo and Gudder: MDF_i is 35 mT for Adzi-Bogdo and 233 mT for Gudder, see Table 3, Fig. 4) may have very similar pressure demagnetization patterns (Fig. 1).

In order to describe how pressure demagnetization affects different coercivity fractions, following Bezaeva et al. (2007, 2010) we calculated a pressure demagnetization parameter ε defined as following:

$$\varepsilon(AF) = [SIRM_{AF}(AF) - IRM_{AFp}(AF)] / SIRM_{AF}(AF) \times 100\% \quad (4),$$

where AF is alternating magnetic field, $SIRM_{AF}$ and IRM_{AFp} are IRM values before and after pressure application, respectively, so that $SIRM_{AF}(AF)$ curve is a curve of AF demagnetization

of SIRM and $IRM_{AFp}(AF)$ is a curve of AF demagnetization of residual IRM after decompression from 1.82 GPa and extraction of the sample from the cell.

Figure 5 displays pressure demagnetization efficiency ε versus AF for 7 samples out of 9, which are discussed below.

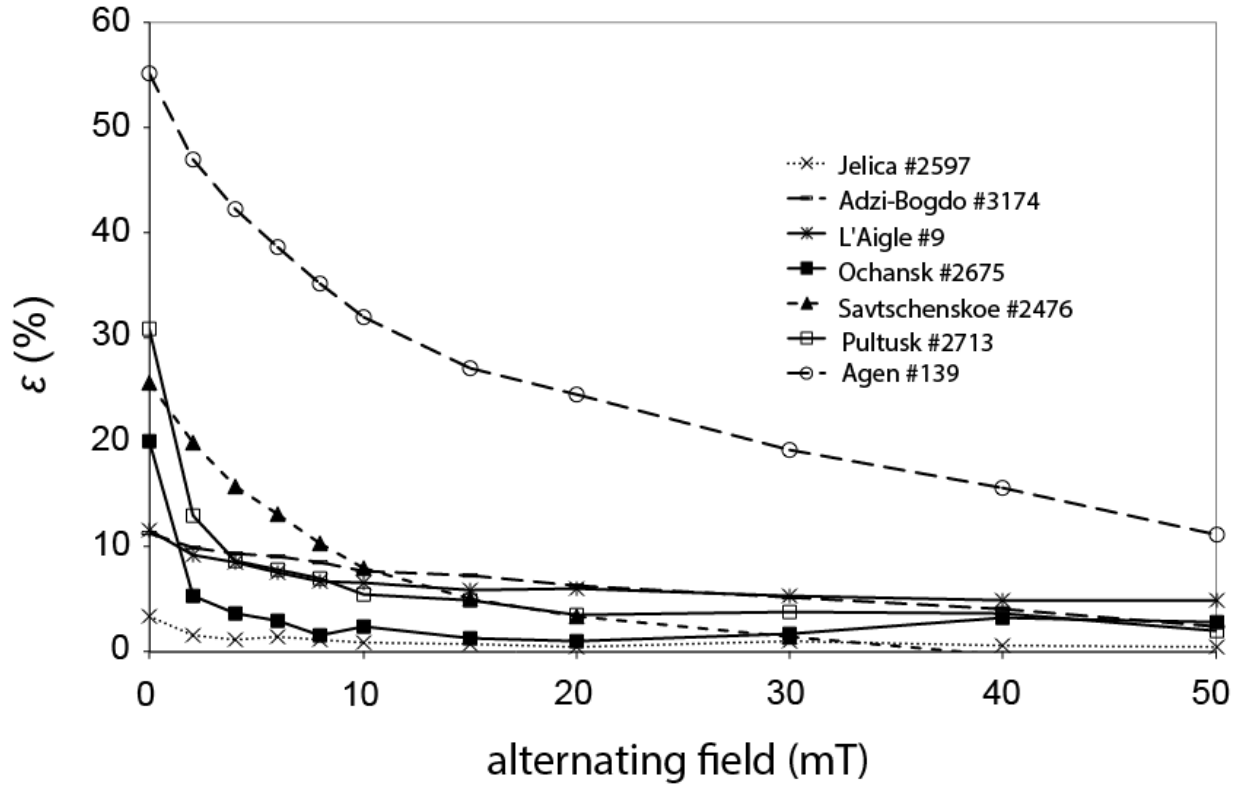


Figure 5. Pressure demagnetization efficiency ε versus alternating magnetic field for the studied ordinary chondrite samples. See equation (4) in the text for the definition of ε .

Table 3 gives the values of $\varepsilon_1 = 1 - \varepsilon(30\text{mT})/\varepsilon_0$ characterizing the shape of $\varepsilon(AF)$ curve. $\varepsilon_0 = \varepsilon(0\text{mT})$. $\varepsilon_1 = 0$ (respectively, $\varepsilon_1 = 1$) if demagnetization affects only grains with coercivity below 30 mT (respectively, above 30 mT). As seen from Fig. 5, for all samples, ε decreases with increasing AF. This indicates that pressure demagnetization preferably affects the lower coercivity fraction, in agreement with previous findings in a pressure range up to 1.24 GPa (Pearce and Karson, 1981; Bezaeva et al., 2007, 2010). However, higher coercivity fractions may also be affected. Indeed, mean $\varepsilon_1 = (73 \pm 17)\%$ is consistent with previous findings for OCs ($\varepsilon_1 = (53 \pm 29)\%$ for pressure demagnetization up to 1.24 GPa, see Bezaeva et al., 2010).

The highest pressure demagnetization efficiency is observed for the magnetically softest meteorites. With an exception of Agen, pressure demagnetization efficiency in the given pressure range drops below 10% above 10 mT for all samples. Then ε_0 decreases with the increase of the magnetic hardness of the samples (Table 3). The only exception is the sample of

Jelica: it has the lowest pressure demagnetization efficiency, which is in agreement with the lowest ε_0 and Δ values, but it has lower MDF_i and B_{cr} values than the samples of l'Aigle and Adzi-Bogdo. It is known that ordinary chondrites often contain a mixture of magnetic minerals (taenite, tetrataenite, kamacite in our case) with different pressure sensitivity (Gattacceca et al., 2014). Thus, one possible explanation of the observed phenomenon is that l'Aigle is likely to contain a small population of magnetically soft grains, which resulted in a higher pressure demagnetization efficiency than what is observed for Jelica. At the same time its hysteresis properties (Table 1) are dominated by magnetically hard population of grains, so that its B_{cr} value is higher than that of Jelica.

Magnetic remanence is known to be more sensitive to deviatoric than hydrostatic loads (Nagata, 1966; Martin and Noel, 1988), so shock waves are likely to produce a larger demagnetization effect than hydrostatic pressure. However, we still can use hydrostatic pressure demagnetization as a rough approximation of shock demagnetization.

This work describes demagnetization of SIRM by hydrostatic pressure in low magnetic field. However, it is important to mention that different types of magnetization (thermoremanent magnetization TRM, anhysteretic remanent magnetization ARM, shock remanent magnetization SRM, viscous remanent magnetization VRM, IRM) may have different pressure sensitivity. Because pressure demagnetization affects preferentially the low coercivity fraction, it is likely that TRM and ARM have a lower but comparable pressure sensitivity than SIRM.

CONCLUSIONS

1. We conducted pressure demagnetization experiments on nine samples of ordinary chondrites (falls only), characterized by a wide range of magnetic hardness quantified by the remanent coercivity B_{cr} in the 5-404 mT range. The experiments revealed that under hydrostatic pressure up to 1.8 GPa, applied in a near-zero ($<5 \mu\text{T}$) magnetic field, ordinary chondrite samples lose up to 51% of their initial saturation isothermal remanent magnetization.
2. The degree of pressure demagnetization is directly proportional to B_{cr} , which is similar to what is observed for other than Fe-Ni ferrimagnetic minerals and in agreement with previous data for Fe-Ni-bearing rocks (Bezaeva et al., 2010). For samples with $B_{cr} > 80 \text{ mT}$, no pressure demagnetization effect is observed under 1.8 GPa. An empirical model allowing the prediction of the degree of pressure demagnetization with 5% accuracy as a function of pressure (up to 1.8 GPa) and B_{cr} is proposed (Fig.2-3).

3. Pressure demagnetization was quantified within coercivity spectrum up to 150 mT: in the given pressure range, pressure demagnetization preferentially affects low coercivity fractions.
4. As the pressure demagnetization curves have concave shape and there is no high-pressure magnetic transition for Fe-Ni metal under 10 GPa, our model at 1.8 GPa can be used for Fe-Ni-bearing meteorites (including but not limited to ordinary chondrites) with shock stage $\leq S1$ (i.e. $p_{\max} \leq 4-5$) GPa [Stöffler et al., 1991]) for Δ estimations within 2 to 5 GPa pressure range. Thus, meteorites with S1 shock stage are likely to have preserved a significant part of the primary (pre-shock) remanent magnetization.

Acknowledgements: This work was supported by RFBR grant no. 18-55-15014 and by CNRS PRC French program. This study was a partial contribution to research theme of Vernadsky Institute of Geochemistry and Analytical Chemistry RAS. We are grateful to MNHN (Paris, France) for the loan of meteorite samples. We thank two anonymous reviewers for their constructive and timely reviews, which helped to improve the manuscript.

REFERENCES

- N. Abreu (ed.), *Primitive Meteorites and Asteroids: Physical, Chemical, and Spectroscopic Observations Paving the Way to Exploration*, 1st edition (Elsevier, Amsterdam, 2018).
- D. D. Badyukov, N. S. Bezaeva, P. Rochette, J. Gattacceca, J. M. Feinberg, M. Kars, R. Egli, J. Raitala, D. M. Kuzina, “Experimental shock metamorphism of terrestrial basalts: Agglutinate-like particle formation, petrology, and magnetism”, *Meteorit. Planet. Sci.* **53** (1), 131-150 (2018).
- N. S. Bezaeva, P. Rochette, J. Gattacceca, R. A. Sadykov, V. I. Trukhin, “Pressure demagnetization of the Martian crust: ground truth from SNC meteorites”, *Geophys. Res. Lett.* **34**, L23202 (2007).
- N. S. Bezaeva, J. Gattacceca, P. Rochette, R. A. Sadykov, and V. I. Trukhin, “Demagnetization of terrestrial and extraterrestrial rocks under hydrostatic pressure up to 1.2 GPa”, *Phys. Earth Planet. Int.* **179**, 7-20 (2010).
- N. S. Bezaeva, N. L. Swanson-Hysell, S. M. Tikoo, D. D. Badyukov, M. Kars, R. Egli, D. A. Chareev, L. M. Fairchild, E. Khakhalova, B. E. Strauss, A. K. Lindquist, “The effects of 10 to >160 GPa shock on the magnetic properties of basalt and diabase”, *Geochem., Geophys., Geosyst.* **17**, 4753-4771 (2016a).

- N. S. Bezaeva, D. A. Chareev, P. Rochette, M. Kars, J. Gattacceca, J. M. Feinberg, R. A. Sadykov, D. M. Kuzina, S. N. Axenov, Magnetic characterization of non-ideal single-domain monoclinic pyrrhotite and its demagnetization under hydrostatic pressure up to 2 GPa with implications for impact demagnetization, *Phys. Earth Planet. Int.* **257**, 79-90 (2016b).
- M. Fuller, F. Rose, P. J. Wasilewski, “Preliminary results of an experimental study of the magnetic effects of shocking lunar soil”, *The Moon* **9**, 57–61 (1974).
- J. Gattacceca, C. Suavet, P. Rochette, B.P. Weiss, M. Winklhofer, M. Uehara, J. Friedrich, “Metal phases in ordinary chondrites: magnetic hysteresis properties and implications for thermal history”, *Meteorit. Planet. Sci.* **49**, 652-676 (2014).
- S. A. Gilder, M. Le Goff, “Systematic pressure enhancement of titanomagnetite magnetization”, *Geophys. Res. Lett.* **35**, L10302 (2008).
- H. Kinoshita, “Studies on piezo-magnetization (III) PRM and relating phenomena”, *J. Geomagn. Geoelectr.* **20**, 155–167 (1968).
- A. S. Kirichenko, A. V. Kornilov, V.M. Pudalov, “Properties of polyethylsiloxane as a pressure-transmitting medium” (*in Russian*), *Instrum. Exp. Tech.* **48** (6), 813–816 (2005).
- D. S. Laretta and H. Y. Jr. McSween (eds.), *Meteorites and the early solar system II*, 1st ed. (The University of Arizona Press, Tucson, AZ, 2006).
- R. J. Martin and J. S. Noel, “The influence of stress path on thermoremanent magnetization”, *Geophys. Res. Lett.* **15**, 507–510 (1988).
- T. Nagata, “Main characteristics of piezo-magnetization and their qualitative interpretation”, *J. Geomagn. Geoelectr.* **18**, 81–97 (1966).
- T. Nagata and H. Kinoshita, “Studies on Piezo-Magnetization (I) Magnetization of Titaniferous Magnetite under Uniaxial Compression”, *J. Geomag. Geoelectr.* **17** (2), 121-135 (1965).
- T. Nagata, M. Funaki, and J. R. Dunn, “Piezomagnetization of meteorites”, *Mem. Natl Inst. Polar Res., Spec. Issue* **25**, 251-259 (1982).
- G. W. Pearce, J. A. Karson, On pressure demagnetization, *Geophys. Res. Lett.* **8**, 725–728 (1981).
- R. A. Sadykov, N. S. Bezaeva, A.I. Kharkovskiy, P. Rochette, J. Gattacceca, V.I. Trukhin, “Nonmagnetic high pressure cell for magnetic remanence measurements up to 1.5 GPa in a SQUID magnetometer”, *Rev. Sci. Instr.* **79**, 115102 (2008).
- R. A. Sadykov, N. S. Bezaeva, P. Rochette, J. Gattacceca, S. N. Axenov, V. I. Trukhin, “Nonmagnetic high pressure cell for measurements weakly magnetic rock samples up to 2 GPa in a superconducting quantum interference device magnetometer”, *Proceedings of the*

- 10th Conference “Physical-Chemical and Petrophysical Researches in Earth’s Sciences”, 305-306 (2009).
- D. Stöffler, K. Keil, and E. R. D. Scott, “Shock metamorphism of ordinary chondrites”, *Geochim. Cosmochim. Acta* **55**, 3845–3867 (1991).
- N. Sugiura and D. W. Strangway, “Magnetic studies of meteorites”, In *Meteoritics and the Early Solar System*, Ed. by J. F. Kerridge and M. S. Mathews (AZ: The University of Arizona Press, Tucson, 1988), pp. 595–615.
- Q. Wei and S. A. Gilder, “Ferromagnetism of iron under pressure to 21.5 GPa”, *Geophys. Res. Lett.* **40** (19), 5131-5136 (2013).
- Q. Wei, C. McCammon, and S. A. Gilder, “High-Pressure Phase Transition of Iron: A Combined Magnetic Remanence and Mössbauer Study”, *Geophys. Geochem. Geosyst.* **18** (12), 4646-4654 (2017).
- B. P. Weiss, J. Gattacceca, S. Stanley, P. Rochette and U. R. Christensen, “Paleomagnetic Records of Meteorites and Early Planetary Differentiation”, *Space Sci. Rev.* **152**, 341–390 (2010).